Muhammed Zakir Tufan*, Birol Üner[1]

Analysis of Heat-Treated Taurus Cedar *(Cedrus libani)* Wood Surface Properties with Fourier Transform Infrared (FTIR) Spectroscopy and Contact Angle Measurement

Analiza svojstava površine toplinski obrađenog drva libanonskog cedra (*Cedrus libani*) uz pomoć Fourierove infracrvene spektroskopije (FTIR) i mjerenja kontaktnog kuta

ORIGINAL SCIENTIFIC PAPER
Izvorni znanstveni rad
Received – prispjelo: 12. 2. 2025.
Accepted – prihvaćeno: 14. 5. 2025.
UDK: 630*84; 674.04
https://doi.org/10.5552/drvind.2025.0251

ABSTRACT • *This study examined the changes in the chemical properties of heat-treated cedar (Cedrus libani) wood as a function of four different treatment temperatures (120, 150, 180 and 210 °C) and three different treatment durations (2, 5 and 8 hours). Particular emphasis was placed on the changes observed in the 1740 cm*$^{-1}$ *carbonyl absorption band in the FTIR spectra of the esterification reaction products, which occurred at 120, 180 and 210 °C for 2, 5 and 8 hours. Surface energies of the samples were also calculated using Young's equation and contact angle measurements with three different liquids: water, glycerol, and hexane. Subsequently, the surface free energies were analyzed using the Lifshitz-van der Waals/acid-base (LW-AB) approach. FTIR analysis indicated that esterification reactions occurred more intensely at temperatures between 180 °C and 210 °C. Contact angle measurements revealed a decrease in polarity and a corresponding increase in non-polarity with increasing heat treatment temperature and duration. Free surface energy analysis demonstrated an increase in the LW component in cedar wood samples treated at 120, 180 and 210 °C for all treatment durations (2, 5 and 8 hours), indicating that surface modification had occurred. These results suggest an increase in nonpolar effects within the surface energy components of the samples, resulting in increased hydrophobicity.*

KEYWORDS: *heat treatment; FTIR; contact angle measurement; cedrus libani; surface energies*

SAŽETAK • *U ovoj studiji predstavljeno je istraživanje promjena kemijskih svojstava toplinski obrađenog drva libanonskog cedra (Cedrus libani) pri četiri različite temperature (120, 150, 180 i 210 °C) i tri različita trajanja obrade (dva, pet i osam sati). Poseban je naglasak stavljen na promjene karbonilne apsorpcijske vrpce na 1740*

---

* Corresponding author

[1] Authors are researchers at Isparta University of Applied Sciences, Department of Forest Products Engineering, Isparta, Turkey. https://orcid.org/0000-0002-6110-7018, https://orcid.org/0000-0001-9249-7402

cm^{-1} u FTIR spektrima produkata reakcije esterifikacije pri temperaturi obrade 120, 180 i 210 °C tijekom dva, pet i osam sati. Također, izračunane su površinske energije uzoraka uz pomoć Youngove jednadžbe i mjerenja kontaktnog kuta trima različitim tekućinama: vodom, glicerolom i heksanom. Nakon toga, slobodne su površinske energije analizirane primjenom Lifshitz-van der Waals/acid-base (LW-AB) pristupa. FTIR analiza pokazala je da su reakcije esterifikacije intenzivnije pri temperaturama između 180 i 210 °C. Mjerenjima kontaktnog kuta otkriveno je da se s povećanjem temperature i trajanjem toplinske obrade smanjuje polarnost i povećava nepolarnost uzoraka. Analiza slobodne površinske energije pokazala je povećanje LW komponente na uzorcima cedrovine obrađenima na 120, 180 i 210 °C za sva tri trajanja obrade (dva, pet i osam sati), što upućuje na to da je nastala modifikacija površine. Ti rezultati potvrđuju povećanje nepolarnih učinaka unutar komponenata površinske energije uzoraka, što rezultira povećanom hidrofobnošću toplinski obrađenog drva.

KLJUČNE RIJEČI: *toplinska obrada; FTIR; mjerenje kontaktnog kuta; libanonski cedar; površinska energija*

1 INTRODUCTION
1. UVOD

Wood, a sustainable material, has been an important raw material for centuries and has been used in many different fields. It is widely used in construction and decoration, especially due to its high strength properties compared to its weight. However, some disadvantageous properties of wood have limited its use in certain applications. Researchers have developed various methods to eliminate or minimize these limitations. Among these methods, chemical treatment, heat treatment and impregnation are the most important ones (Kocaefe *et al.*, 2007; Hill, 2011; Bal, 2013; Sivrikaya *et al.*, 2015a; Svenson *et al.*, 2023).

The processes carried out to change or improve the disadvantages of wood material such as its sensitivity to moisture, low levels of dimensional stability, low hardness, limited resistance to abrasion, fungi, termites and UV radiation are generally referred to as “wood modification”. The modification process causes permanent changes in the chemical structure of wood (Altınok *et al.*, 2010; Sandberg *et al.*, 2017; He *et al.*, 2023). The fact that heat treatment, which is one of the modification methods, is commercially applicable and accepted as environmentally friendly makes it stand out. With heat treatment, permanent changes are created especially in the chemical structure of the polymeric structure that forms the wood, making the material more resistant to the mentioned disadvantages (Korkut *et al.*, 2008; Esteves and Pereira, 2008; Korkut and Kocaefe, 2009; He *et al.*, 2023).

The main objective of heat treatment is to alter the chemical structure so as to reduce hygroscopicity and improve wood properties. During this process, chemical modifications occur, including the degradation of hemicelluloses and the esterification of hydroxyl groups, which decrease the number of accessible OH groups, thereby reducing wood swelling and shrinkage (Gerardin *et al.*, 2007; Kocaefe *et al.*, 2008; Hill *et al.*, 2021; Čabalová *et al.*, 2022). As a result of heat treatment, increases in lignin content, decay resistance, and dimensional stability have been observed, while mechanical properties and water absorption capacity tend to decrease. Additionally, improvements in resistance to weathering have been reported (Bal, 2013; Tufan *et al.*, 2022).

Although most of the free and bound water is lost from wood up to 150 °C, some of the water bound to the cell wall continues to remain up to higher temperatures (Gezici-Koç *et al.*, 2017; Penvern *et al.*, 2020; Aydın, 2021; Hill *et al.*, 2021). At temperatures higher than 150 °C, heat treatment chemical processes speed up (Boonstra, 2008; Piernik *et al.*, 2022). The range between 160 and 240 °C is typical for heat treatment (Militz, 2002; Sikora *et al.*, 2018). According to Kamdem *et al.* (2002) and Hill (2007), the process temperature and duration vary from 180 to 280 °C and 15 to 24 hours, respectively, depending on the type of wood, sample size, moisture content, desired mechanical performance, resistance to biological factors, and desired properties like stability.

FTIR is an easy and nondestructive analytical˝tool for determining changes in the chemistry of wood structure due to modification (Chien *et al.*, 2018; Peng *et al.*, 2022). Because of these characteristics, its importance and areas of use have grown. FTIR analysis gives important information about the changes in the O-H, C-H, N-H, and C-O groups of cellulose structures and intra- and inter-chain hydrogen bonds. Thus, it provides more detailed information about the interactions of the polymer components of wood material at the molecular level (Cherdkeattikul *et al.*, 2020; Kaya *et al.*, 2021).

In the literature, heat treatment has been applied to many different types of wood. The changes that occur as a result of these processes have been investigated in detail. Most of the studies have focused on these types, especially due to the durable and aesthetic structures of cedar wood species. For example, as a result of 1 and 2 hours of heat treatment at 220 °C on western red cedar samples, it was determined that pits formed in the tracheid walls, ray parenchyma and pit aspiration of the wood material (Awoyemi and Jones, 2011). In the study conducted on eastern red cedar wood samples, a decrease in the shear and hardness values of the samples occurred as a result of the heat treatment applied at 120 °C. It was concluded that the sample surface roughness improved when the temperature increased and time was kept constant. Also, a decrease was reported in the water absorption values, swelling ratio and diffusion coefficient of samples depending on these parameters (Dilik and Hiziroglu, 2012; Kasemsiri *et al*., 2012).

Thermally treating the wood leads to substantial alterations in color, chemical composition, dimensional stability and biological resistance of the materials, depending on the treatment temperature and duration. Jimenez *et al*. (2011) found that coloration of Malapapaya (*Polyscias nodosa*) wood changed from yellowish to dark brown when processed at various temperatures. Similarly, Barcik *et al*. (2015) showed that temperature significantly facilitated the darkening of oak and Scots pine, while the darkening effect was slightly more pronounced in birch. When studying changes in chemical structure, Srinivas and Pandey (2012) reported a decrease in the content of hydroxyl groups with heat treatment of rubbberwood and silver oak which affected the hygroscopicity of the material. Likewise, Xu *et al*. (2019) also reported that the amount of hydroxyl groups decreased, while the carbonyl groups increased, with increasing temperature in white oak (*Quercus alba*).

In terms of dimensional stability, Builes *et al*. (2021) found that the dimensional stability of Pinus oocarpa (*ocote pine*) wood was increased by heat treatment as a result of the removal of hydroxyl groups. Similarly, Wang *et al*. (2018) also found a relationship between the decrease in the effective free hydroxyl group content and the decrease in the immobilized free water content, which led to a decrease in the equilibrium moisture content and thus increased the dimensional stability in Masson pine (*Pinus massoniana*). Bytner *et al*. (2021) also noted that the equilibrium moisture content and water uptake rate of black poplar (*Populus nigra*) wood were reduced by heat treatment. Similarly, Durmaz *et al*. (2019) showed that, although the compressive and flexural strengths of Scots pine (*Pinus sylvestris*) were reduced by heat treatment, the dimensional stability was significantly increased. In terms of biological durability, Altgen *et al*. (2020) reported that thermal degradation of hemicelluloses in Scots pine increased the resistance to brown rot fungi. Additionally, Vidholdova *et al.* (2022) showed that higher temperature heat treatment greatly improved the decay resistance of Norway spruce (*Picea abies*) wood against brown rot and white rot fungi.

According to some studies, the increased surface roughness formed during heat treatment in the range of 200-220 °C is the result of the combined effects of thermal stresses, hemicellulose degradation, lignin rearrangement and structural irregularities (Nabil *et al*., 2018; Hill *et al*., 2021; Wu *et al*., 2021; Mastouri *et al*., 2023). It was found that cracks occurred in the samples and the presence of these cracks decreased the compressive, flexural and tensile strengths of the heat-treated samples of Deodar cedar (*Cedrus deodara*) wood (Oliveira *et al*., 2022). According to the obtained data, its resistance against decaying of wood material was increased by applying it on Japanese cedar (*Cryptomeria japonica*). Another study showed that, when Japanese cedar (*Cryptomeria japonica*) samples were subjected to heat treatment at 20, 40, 60, 80, and 100 °C, the highest compression strength, yield stress, and Young's modulus were obtained at 20 °C, while these values decreased at 100 °C (Chang *et al*., 2019; Toba *et al*., 2024). However, the majority of these studies have focused on different cedar species, and research conducted on Lebanon Cedar/Toros Cedar (*Cedrus libani)* is quite limited.

In recent years, the production and use of heat-treated wood have increased significantly in the wood industry. This process, which is widely used in certain tree species, has been applied to cedar wood, which is widely distributed in the Mediterranean region and used for various purposes, but detailed information about the chemical changes that occur is still limited. Considering this deficiency, the chemical changes of Taurus cedar (*Cedrus libani*) wood after heat treatment were investigated. While previous studies have mainly focused on other coniferous species, especially Cedrus atlantica and Cedrus deodara, this study aims to fill this gap by investigating a coniferous species of significant regional importance. The study provides information not only on the general changes of functional groups, but also on the quantitative changes in specific bonds, such as carbonyl groups around 1740 cm^{-1}, with respect to temperature and time, as shown by FTIR measurements. Furthermore, by using surface contact angle measurements to relate these chemical changes, a comprehensive explanation of the effect of heat treatment on the hydrophilicity and hydrophobicity surface properties was provided.

2 MATERIALS AND METHODS
2. MATERIJALI I METODE

Cedar log samples were selected at 1-meter and 3-meter intervals from a cutting area under the jurisdiction of the Burdur-Bucak Forest Management Directorate. These samples were cut into 50 cm lengths and prepared from the sapwood portions. The cedar samples were air-dried and then processed to dimensions of (22 × 70 × 350) mm^3. Heat treatment was conducted at four different temperatures (120 °C, 150 °C, 180 °C, and 210 °C) and for three different durations (2 hours, 5 hours, and 8 hours). The heat treatment conditions were established taking into consideration the range of temperature and time available in the literature. The hemicellulose starts to degrade at around 140 °C and then the cellulose structure changes (Esteves *et al*., 2007; Rowell *et al*., 2009). It is known that temperatures of 240 °C and beyond can result in the deterioration of mechanical properties of wood (Hill *et al*., 2021; Adhikari *et al*., 2025). Thus, in the current study, the lowest treatment temperature was selected at 120 °C to study possible structural differences at a temperature lower than 140 °C and the highest temperature was 210 °C to prevent substantial mechanical damage.

To evaluate the effect of temperature and time relationship on the material, 2, 5 and 8 h treatment times were selected (Hill *et al*., 2007; Esteves *et al*., 2007; Esteves and Pereira, 2009; Hill *et al*., 2021; Adhikari *et al*., 2025). A 2 h time period was selected to obtain rapid improvement at high temperatures, while a 5 h time period was determined for the best improvement at medium temperatures. On the other hand, an 8 h time period was selected to monitor the early stage of chemical changes at low temperatures.

The treatment was performed using a laboratory furnace (FN 500, Nüve Co., Ankara, Turkey) capable of maintaining temperatures within ± 1 °C in an ambient air environment (Figure 1). Control samples were also prepared for each temperature group and evaluated under the same conditions. Following heat treatment, all test samples were conditioned at 65 % relative humidity and 20 °C.

2.1 FTIR analysis
2.1. FTIR analiza

FTIR spectroscopy was used to determine the chemical changes occurring in the heat-treated cedar samples compared to the control samples. With the help of this analysis, changes in the structural composition of cedar wood samples as a result of heat treatment were investigated. It was determined that the changes occurred in parallel with the disintegration of amorphous cellulose (decomposition temperature 200-240 °C) and irregular structures of hemicelluloses in the structure of the samples, resulting in an increase in the crystallinity of cellulose (Yang *et al*., 2016; Chang *et al*., 2019). In this change, since the amount of cellulose remained unchanged, a proportional increase in the crystallinity of cellulose occurred. These increases can only be explained by the decrease in amorphous regions. The effects of this change on the OH groups and cellulose crystal structures in the cedar samples were investigated in detail by FTIR spectroscopy.

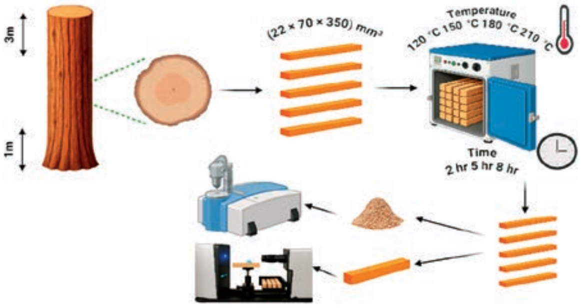

Figure 1 Heat treatment application process and performance tests
Slika 1. Postupak toplinske obrade i ispitivanja svojstava cedrovine

Functional group analysis was performed using IR Prestige-21 model FTIR spectrometer (Shimadzu Corp, Japan). For this analysis, samples were prepared as solid powder mixed with KBr and pressed into pellets. Specifically, the samples were ground with KBr in an agate mortar and subsequently pressed into tablets at 10 bar pressure. Since KBr is outside the visible region, the obtained spectra are attributed solely to the sample. Spectra were acquired by averaging 10 scans over the range of 4000-400 cm^{-1}. These spectra were then normalized at 2950 cm^{-1}.

2.2 Contact angle measurement
2.2. Mjerenje kontaktnog kuta

Contact angle measurements typically employ droplet volumes ranging from 0.5 to 10 µL to minimize gravitational deformation. Variations in droplet volume can influence measurement results due to the combined effects of gravity and droplet size. While 2-3 µL droplets are often ideal for contact angle measurements, the low water retention of superhydrophobic surfaces can hinder the deposition of droplets smaller than 4 µL. For accurate measurements, it is crucial to perform readings immediately after droplet deposition to prevent evaporation. Simultaneously, allowing a brief period for droplet spreading and interaction with the surface is also essential (Zhang *et al*., 2004; Ferrari *et al*., 2006; Tianyi and Jiang, 2018). Accordingly, contact angle measurements of the cedar samples were performed by capturing images every 5 seconds for 30 seconds after a 5 µL water droplet was placed on the surface.

In this study, mechanical cutting was applied to equalize the surface roughness of the samples. Surface free energy is theoretically defined for ideal and smooth surfaces. However, real surfaces can deviate from the ideal due to factors such as roughness, contamination, and heterogeneity. Such surface characteristics can affect the measured contact angles, leading to uncertainties reflected in surface free energy calculations (Gindl *et al*., 2001; Qin *et al*., 2015). In this context, the surface free energy values obtained in this study should be evaluated not as absolute values, but only as a tool for relative comparison between measurements performed under the same experimental conditions.

Samples were prepared using the sessile drop method on an Attention instrument in accordance with the TAPPI T558 om-97 (Canada) standard (TAPPI). Cedar samples with dimensions of (22 × 70 × 350) mm³ (tangential × radial × longitudinal) were used to measure contact angles. The contact angles of both control and heat-treated samples were measured using water, hexane, and glycerol (hexane and glycerol were supplied by Labor Teknik, Isparta, Turkey). Initially, ten drops of water were placed on each sample to determine the water contact angle. This procedure was then repeated using hexane and glycerol. Subsequently, comparisons were made between the control and heat-treated samples, and changes in surface properties and surface free energy were analyzed.

2.2.1 Young's equation
2.2.1. Youngova jednadžba

According to Young's equation (1), the relationship between contact angles and surface free energy of cedar wood samples was calculated (Gerardin *et al.*, 2007; Zhao and Jiang, 2018).

$$\cos\theta = \frac{\gamma_{\mathrm{gs}} - \gamma_{\mathrm{ls}}}{\gamma_{\mathrm{gl}}} \qquad (1)$$

In the equation, cos θ represents the contact angle, γ_{gs} represents the gas-solid surface free energy, γ_{ls} represents the liquid-solid surface free energy and γ_{gl} represents the gas-liquid surface free energy.

2.2.2 Lifshitz-van der Waals and acid-base approach
2.2.2. Lifshitz-van der Waals i kiselo-bazni pristup

Lifshitz-van der Waals/acid-base (LW-AB) approach was applied using the contact angle values and surface free energy data of water, hexane and glycerol. Thanks to this approach, it was determined whether the surface free energies of cedar wood samples show polar or apolar properties. It also allowed a detailed examination of the changes in the acidic-basic components. All these analyses were carried out using Eq. 2, Eq. 3 and Eq. 4. (Gerardin *et al.*, 2007; Chen *et al.*, 2020).

$$\gamma_{\mathrm{sl}}^{\mathrm{LW}} = \left(\sqrt{\gamma_{\mathrm{lv}}^{\mathrm{LW}}} - \sqrt{\gamma_{\mathrm{sv}}^{\mathrm{LW}}}\right)^2 \qquad (2)$$

$$\gamma_{\mathrm{sl}}^{\mathrm{AB}} = 2\left(\sqrt{\gamma_{\mathrm{sv}}^{+}\cdot\gamma_{\mathrm{sv}}^{-}} + \sqrt{\gamma_{\mathrm{lv}}^{+}\cdot\gamma_{\mathrm{lv}}^{-}} - \sqrt{\gamma_{\mathrm{sv}}^{+}\cdot\gamma_{\mathrm{lv}}^{-}} - \sqrt{\gamma_{\mathrm{sv}}^{-}\cdot\gamma_{\mathrm{lv}}^{-}}\right) \qquad (3)$$

$$(1+\cos\theta)\cdot\gamma_{\mathrm{lv}} = 2\left(\sqrt{\gamma_{\mathrm{sv}}^{\mathrm{LW}}\cdot\gamma_{\mathrm{lv}}^{\mathrm{LW}}} + \sqrt{\gamma_{\mathrm{sv}}^{+}\cdot\gamma_{\mathrm{lv}}^{-}} + \sqrt{\gamma_{\mathrm{sv}}^{-}\cdot\gamma_{\mathrm{sv}}^{+}}\right) \quad (4)$$

Here, cosθ represents the cosine of the contact angle; γ^{LW} represents the Lifshitz-van der Waals surface free energy; γ^{AB} represents the acid-base surface free energy; γ_{SV} represents the solid-gas surface free energy; γ_{lv} represents the liquid-gas surface free energy; γ^{+} represents the acidic (electron acceptor) component of the surface free energy; and γ^{-} represents the basic (electron donor) component of the surface free energy.

3 RESULTS AND DISCUSSION
3. REZULTATI I RASPRAVA

3.1 FTIR analysis
3.1. FTIR analiza

The wavenumber in the 1800-800 cm^{-1} range represents the stretching and bending vibrations between molecules. FTIR examines the changes in absorption bands related to cellulose, lignin and hemicelluloses in this range (Kubovsky *et al.*, 2020). In this study, FTIR analyses of cedar wood samples subjected to heat treatment at different temperatures (120 °C, 180 °C and 210 °C) and durations (2, 4, 6 and 8 hours) were per-

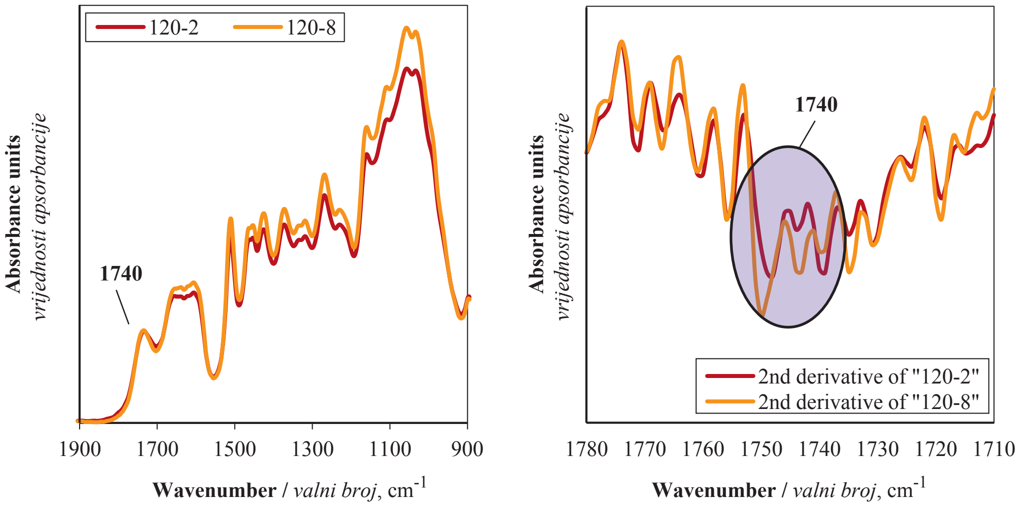

a) b)

Figure 2 Shows (a) FTIR spectra and (b) second derivative spectra of the 1740 cm^{-1} absorption band for cedar samples heat-treated at 120 °C for 2 and 8 hours
Slika 2. Prikaz (a) FTIR spektara i (b) spektara druge derivacije apsorpcijske vrpce 1740 cm^{-1} uzoraka toplinski obrađene cedrovine na 120 °C tijekom dva i osam sati

formed. Depending on temperature and duration, one mole of water is removed from alcohol and ether molecules during heat treatment, leading to esterification (Tjeerdsma and Militz, 2005). To explore in detail, the changes in the ester structure that occur because of the OH groups that are eliminated from the environment as a result of the heat treatment, the second derivative of the 1740 cm^{-1} carbonyl absorption band was obtained. Additionally, the time-dependent variations in absorbance values at the wavelengths of 1600, 1500, 1460, 1420, 1373, 1318, 1267, 1160, and 1032 cm^{-1} are presented in Table 1.

As noted by Esteves *et al*. (2013) and Gaff *et al*. (2023), the FTIR is also an important technique to reveal the variations of characteristic functional groups (in particular, in the 1750-1700 cm^{-1} range, carbonyl and ester groups, ketones, aldehydes and carboxylic acids) in the composition of lignin and hemicelluloses. Additionally, the 1740 cm^{-1} absorption band sensitive to structural variation changes that occur in several modifications of different functional groups e.g., esterification, was also detected in this work (Figure 2a; Hou and Wu, 2019). In the research, the differences that resulted from heat-treated samples at 120 °C during a period of time were analyzed. This was done based on the absorbance values of 0.856 (2 hours) and 0.872 (8 hours), which were the numbers resulting from this study. These data were not found to be statistically significant. Also, these findings were verified by previous research. Tjeerdsma and Militz (2005) proved that thermal treatment of the temperatures higher than 185 °C changes the rates of the esterification processes significantly. In the study conducted by Esteves *et al.* (2013), it was stated that the 1740 cm^{-1} absorption band was minimally affected by heat treatment at 170 °C.

The C = C stretching vibrations in the aromatic rings in the lignin structure were attributed to the absorption band at 1600 cm^{-1}. Therefore, the indicated absorption band indicates the presence of ring structures and unsaturated bonds in that region (Gaff *et al*., 2023; Qian *et al*., 2024). The analysis revealed the intensity of the absorption band is slightly rising as the duration of treatment of constant temperature increases. Factors of this effect include the increase in the production of conjugated carbonyl groups, condensed lignin processes, and carboxylation of polysaccharides (González-Peña *et al*., 2009, Kubovsky *et al*., 2020, Li *et al*., 2024).

The absorption band at 1500 cm^{-1} corresponds to the stretching vibrations of the benzene ring and the C=C vibrations of the aromatic skeleton characteristic of the lignin structure (Kubovsky *et al*., 2020). At constant temperature, an increase in absorption values occurred due to the increase in heat treatment time. The increases are due to improvements in the chemical structure of the wood material. The increase in lignin content occurred due to the degradation of amorphous carbohydrates in hemicellulose structures and structural changes in the guaiacyl and syringyl units of lignin in wood structures (Li *et al*., 2015). Also, in another study, C=C aromatic stretching vibrations in the lignin structure were reported to be responsible for the 1505 cm^{-1} region. Furthermore, the study authors speculated that the growth occurred here due to the loss of extractive compounds and carbohydrates from the structure more than because of this wavelength (Moosavinejad *et al*., 2019).

Table 1 Variation of FTIR spectroscopy absorbance values with wavenumber (cm^{-1}) under different temperature and time conditions

Tablica 1. Varijacije apsorbancije FTIR spektroskopije s valnim brojem (cm^{-1}) pri različitim temperaturnim i vremenskim uvjetima

Temperature *Temperatura*	**Wavenumber** / V*alni broj,* cm^{-1}								
	1600	1500	1460	1420	1373	1318	1267	1160	1032
120 °C	2 hour 1.225	2 hour 1.379	2 hour 1.752	2 hour 1.809	2 hour 1.897	2 hour 1.788	2 hour 2.175	2 hour 2.574	2 hour 3.360
	8 hour 1.317	8 hour 1.495	8 hour 1.865	8 hour 1.956	8 hour 2.048	8 hour 1.938	8 hour 2.374	8 hour 2.836	8 hour 3.728
120 °C	2 hour 1.225	2 hour 1.379	2 hour 1.752	2 hour 1.809	2 hour 1.897	2 hour 1.788	2 hour 2.175	2 hour 2.574	2 hour 3.360
180 °C	2 hour 1.521	2 hour 1.786	2 hour 2.203	2 hour 2.265	2 hour 2.382	2 hour 2.283	2 hour 2.823	2 hour 3.359	2 hour 3.397
210 °C	2 hour 0.764	2 hour 0.803	2 hour 1.013	2 hour 1.073	2 hour 1.141	2 hour 1.099	2 hour 1.262	2 hour 1.493	2 hour 1.503
120 °C	8 hour 1.317	8 hour 1.495	8 hour 1.865	8 hour 1.956	8 hour 2.048	8 hour 1.938	8 hour 2.374	8 hour 2.836	8 hour 3.728
180 °C	8 hour 1.521	8 hour 1.646	8 hour 2.049	8 hour 2.120	8 hour 2.270	8 hour 2.222	8 hour 2.697	8 hour 3.266	8 hour 4.412
210 °C	8 hour 0.887	8 hour 0.829	8 hour 1.085	8 hour 1.135	8 hour 1.246	8 hour 1.231	8 hour 1.378	8 hour 1.654	8 hour 2.137

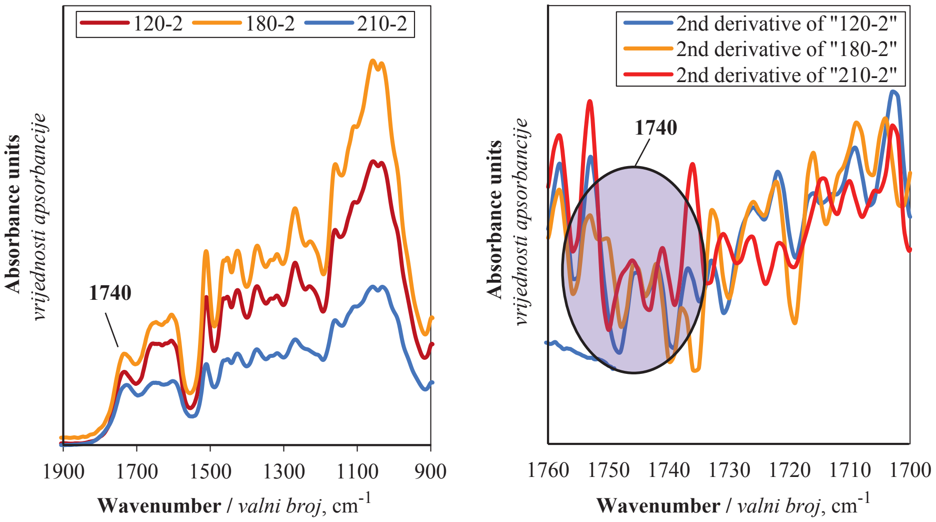

a) b)

Figure 3 Shows (a) FTIR spectra of cedar wood samples heat-treated at 120, 180, and 210 °C for 2 hours, and (b) the second derivatives of the 1740 cm^{-1} absorption band of the same samples

Slika 3. Prikaz (a) FTIR spektara toplinski obrađenih uzoraka cedrovine na 120, 180 i 210 °C tijekom dva sata i (b) drugih derivacija apsorpcijske vrpce 1740 cm^{-1} istih uzoraka

The 1460 cm^{-1} absorption band corresponds to the asymmetric C-H deformation vibrations in the lignin matrix (Piernik *et al*., 2022; Godinho *et al*., 2024). Each vibrational interaction leads to the formation of the 1420 cm^{-1} absorption band, for which the increase in absorbance intensity after exposure to heat treatment is observed. The increase in intensity of the 1420 cm^{-1} absorption band can be interpreted to be a result of the enhancement of C-H deformation vibrations in lignin and carbohydrate constituents, while the contribution of an aromatic skeletal vibrations system in lignin structure may lessen due to decomposition. The intensity of this effect has been linked to the duration of thermal treatment (Kacik *et al*., 2016; Jaruwat *et al*., 2018). Moreover, some of the observed spectral changes have been ascribed to chemical processes, including the deactivation of the methoxyl structure and the degradation of the lignin structure (Kubovsky *et al*., 2020).

The CH_2 bending vibrations of cellulose and hemicellulose structures have been linked to the absorption band observed at 1371 cm^{-1} (Caputo *et al*., 2021; Liao *et al*., 2024). In comparing the two cedar wood samples used in the study, it was observed that the intensity of absorption of the absorption band increased with increasing duration of heat treatment. In the 1318 cm^{-1} absorption band, similar increases were seen with extended processing time. Based on these results, higher density structures were formed due to an increase in the material's density (Kubovsky *et al*., 2020).

The C−O stretching vibrations in the guaiacyl ring have been attributed to the absorption band at 1267 cm^{-1}. It has been reported in the literature that for heat-treated wood samples, an increase in absorbed energy values occurs due to an increase in the treatment time at constant temperature. This increase indicates that, unlike for syringyl structures, degradation can take place at lower process temperatures and that the time of heat treatment can also affect this degradation (Kubovsky *et al*., 2020; Varga *et al*., 2020).

The absorption band at 1161 cm^{-1} was attributed to the C-O-C stretching vibrations of cellulose and hemicellulose structures. (Caputo *et al*., 2021). This absorption band has been observed to change markedly with increasing time, particularly for different durations of heat treatment. The increase in absorbance values indicates the occurrence of dehydration processes and the slow degradation of carbohydrate components. Intermolecular or cross-links are made that facilitate the formation of covalent bonds between molecules by these processes to form ether bonds. According to Kubovský and Kačík (2014) and Kačík *et al*. (2016), the absorption band at 1030 cm^{-1} can be attributed to C-O-C stretching vibrations for the primary alcohol functional groups found in the structure of cellulose and hemicellulose, as well as C-O deformation vibrations for the primary alcohol part of cellulose. A gradual change has occurred in the structure of cellulose, one of the most important components of wood material, according to the observed increases in this absorption band (Kubovsky *et al*., 2020; Dassanayake *et al*., 2023).

Analysis of the 1740 cm^{-1} absorption band absorbance values presented in Figure 3a (120 °C-2 hours → 0.856, 180 °C-2 hours → 1.063, 210 °C-2 hours → 0.677) demonstrates a significant variation observed after 2 hours of treatment at 210 °C. This observed change could be attributed to the conjugation of carbonyl groups with other double bonds, such as those found in aromatic or alkene structures, as well as the

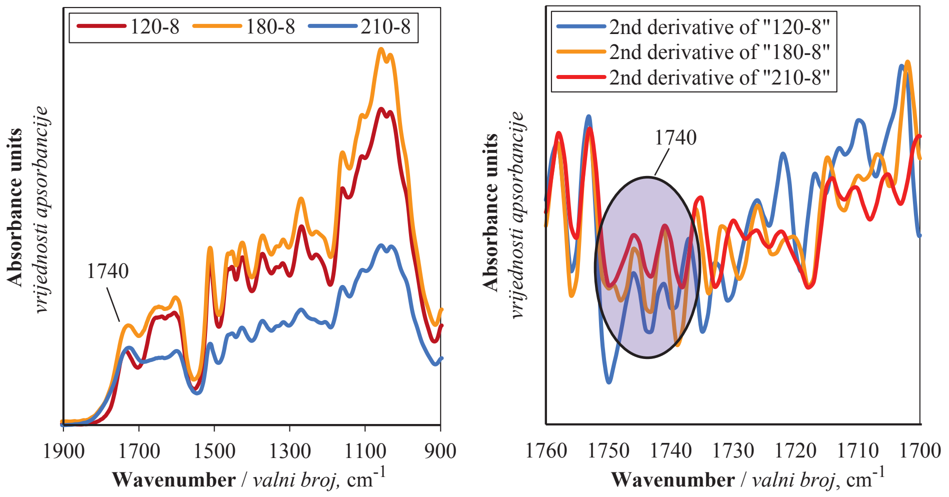

a) b)

Figure 4 Shows FTIR spectra (a) of cedar samples heat-treated at 120, 180, and 210 °C for 8 hours, and (b) the second derivative FTIR spectra of the same samples at the 1740 cm^{-1} absorption band
Slika 4. Prikaz (a) FTIR spektara toplinski obrađenih uzoraka cedrovine na 120, 180 i 210 °C tijekom osam sati i (b) drugih derivacija apsorpcijske vrpce 1740 cm^{-1} istih uzoraka

formation of additional carbonyl or carboxyl groups through oxidation reactions that occur during thermal decomposition processes (Kubovský *et al*., 2020). Furthermore, the existence of ester bonds in aliphatic and aromatic compounds, as well as the modifications that take place in these bonds, might be linked to the alterations observed in the absorption band at 1740 cm^{-1} (Gordobil, 2018).

When the heat treatment time is kept constant, the absorption band at 1600 cm^{-1} (high peak) had the most significant change at 210 °C / 2-hour with the increase in temperature. It was also determined that the 1500 cm^{-1} absorption band underwent similar changes. The 1460 cm^{-1} and 1420 cm^{-1} absorption bands exhibited the same effect after a 2-hour heat treatment at 210 °C. These changes were attributed to the gradual decomposition of lignin components within the material's structure, as well as to the impact of high temperatures on the functional capacity of methoxyl groups (Kubovsky *et al*., 2020).

An important change in absorbance values was noticed within the 1371 cm^{-1} absorption band after the heat treatment at 210 °C for 2 hours while the intensity of the 1318 cm^{-1} absorption band increased with rising temperatures, but a sharp decrease was observed after treatment at 210 °C for 2 hours. The largest change in the 1267 cm^{-1} absorption band occurred at 210 °C / 2-hour heat treatment conditions. These observed changes collectively demonstrate the influence of elevated temperatures on structural density and degradation phenomena.

At the 1160 cm^{-1} absorption band, a substantial modification was evident following the 2-hour treatment at 210 °C. Concurrently, a marked alteration, particularly during the aforementioned 2-hour period at 210 °C, was observed within the 1030 cm^{-1} absorption band. These changes indicate gradual transformations within the cellulose matrix (Kubovsky *et al*., 2020).

The absorbance values for the 1740 cm^{-1} absorption band, as shown in Figure 4a (120 °C-8 hours → 0.872, 180 °C-8 hours → 1.139, 210 °C-8 hours → 0.872), exhibit a significant change in the second derivative spectra (Figure 4b) between 180 °C and 210 °C, over the 8-hour treatment period. While this change is attributed to the increased rate of thermal decomposition at temperatures above 180 °C, the origin of variations in the 1740 cm^{-1} absorption band is debated in the literature. One study suggests that these changes are due to hemicellulose degradation caused by heat treatment (Wang *et al*., 2024), while another attributes the increase in this absorption band to the presence of carbonyl groups (Tuncer *et al*., 2024).

Within the 1600 cm^{-1} absorption band, a marginal increase in absorbance values was evident with increasing temperature over the 8-hour duration. However, the most substantial alteration was observed at 210 °C following an 8-hour treatment. Concurrently, the most significant modification at the 1500 cm^{-1} absorption band was also found to occur at 210 °C after an 8-hour treatment period.

Consistent with the trends observed at the 1460 cm^{-1} and 1420 cm^{-1} absorption bands, the most substantial changes in absorbance within the 1371 cm^{-1}, 1318 cm^{-1}, 1267 cm^{-1}, 1160 cm^{-1}, and 1030 cm^{-1} absorption bands were likewise evident at 210 °C following an 8-hour treatment. Notably, within the 1318 cm^{-1} absorption band, a concomitant increase in intensity was also observed with increasing temperature.

A comparative analysis of the data presented in Figure 5 indicates that the heat treatment protocol main-

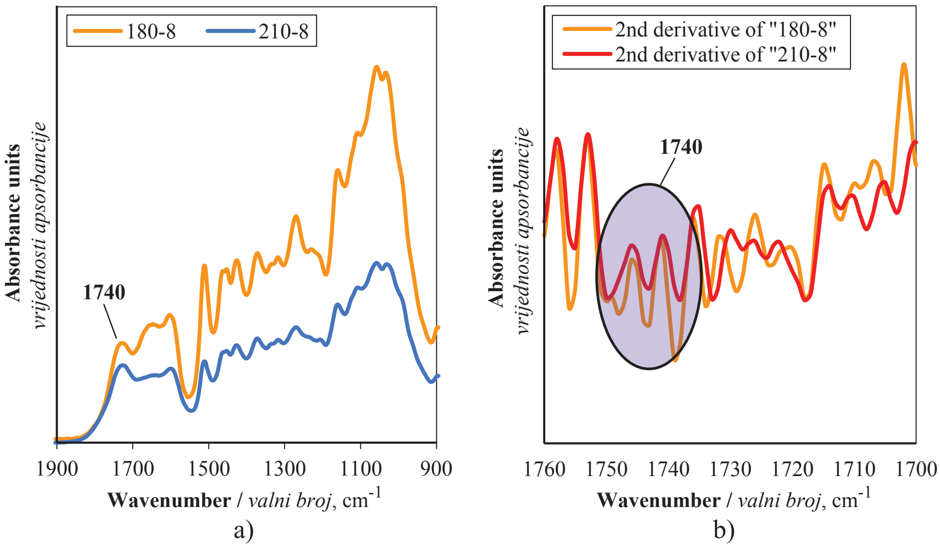

Figure 5 Shows FTIR spectra (a) of cedar samples heat-treated at 180 and 210 °C for 8 hours, and (b) the second derivative FTIR spectra of the same samples at the 1740 cm^{-1} absorption band

Slika 5. Prikaz (a) FTIR spektara toplinski obrađenih uzoraka cedrovine na 180 i 210 °C tijekom osam sati i (b) drugih derivacija apsorpcijske vrpce 1740 cm^{-1} istih uzoraka

tained a constant duration while investigating the influence of increasing temperature on the spectral characteristics of various functional groups. Specifically, the most substantial modifications in both the 1740 cm^{-1} absorption band and its associated second derivative were evident during the 8-hour treatment period spanning 180 to 210 °C. Analogous variations were also observed in other functional groups (Figure 4).

According to Table 2, the heat treatment of cedar wood samples at 120 °C, 180 °C, and 210 °C resulted in various chemical changes, leading to increases and decreases in specific FTIR spectral absorption bands. Table 2 further details the underlying reasons for these observed changes at different temperatures.

As the temperature increased, the intensity of the hydroxyl groups in the 3350 cm^{-1} absorption band decreased due to esterification (Figure 6b). Particularly at 210 °C and short heating durations (2 hours), a significant decrease in the intensity of this absorption band is observed. This reduction can primarily be attributed to

Table 2 Factors influencing increases and decreases in FTIR absorption bands at specific temperatures as a result of heat treatment

Tablica 2. Čimbenici koji utječu na povećanje i smanjenje FTIR apsorpcijskih veza na određenim temperaturama kao rezultat toplinske obrade

Increases in temperatures of 120 °C and 180 °C *Povećanje na temperaturama 120 i 180 °C* (Zhu *et al*., 2016; Zhang *et al*., 2017; Li *et al*., 2017; Sikora *et al*., 2018; Aytin *et al*., 2022; Zhang *et al*., 2023; Lyu *et al*., 2024)	**Reductions in temperatures of 180 °C and 210 °C** *Smanjenje na temperaturama 180 i 210 °C* (Esteves and Pereira, 2009; Wang *et al*., 2016; Candelier *et al*., 2016; Výbohová *et al*., 2018; Kubovský *et al*., 2020; Piernik *et al*., 2022; De Ligne *et al*., 2024)
As the material becomes more crystalline, certain vibrational modes may become more regular, leading to stronger absorption. *Kako materijal postaje kristalniji, određeni vibracijski modovi mogu postati pravilniji, što dovodi do jače apsorpcije.*	The degradation of lignin, hemicellulose, and cellulose can lead to material loss, resulting in a decrease in the intensity of the functional groups responsible for the observed peaks. *Razgradnja lignina, hemiceluloze i celuloze može dovesti do gubitka materijala, što rezultira smanjenjem intenziteta funkcionalnih skupina odgovornih za uočene vrhove.*
Oxidation reactions or other chemical changes can result in the formation of new light-absorbing functional groups in the analyzed region. *Oksidacijske reakcije ili druge kemijske promjene mogu rezultirati stvaranjem novih funkcionalnih skupina koje apsorbiraju svjetlost u analiziranom području.*	Some degradation products may be volatile and migrate away from the sample, contributing to further attenuation of the signal. *Neki produkti razgradnje mogu biti hlapljivi i udaljiti se od uzorka, pridonoseći daljnjem slabljenju signala.*
The removal of water molecules as the material dries may enable other functional groups to produce more prominent signals. *Uklanjanje molekula vode dok se materijal suši može omogućiti drugim funkcionalnim skupinama da proizvode jače signale.*	At high temperatures, the material may undergo charring, resulting in major spectral changes. *Na visokim temperaturama materijal se može pougljeniti, što rezultira velikim spektralnim promjenama.*

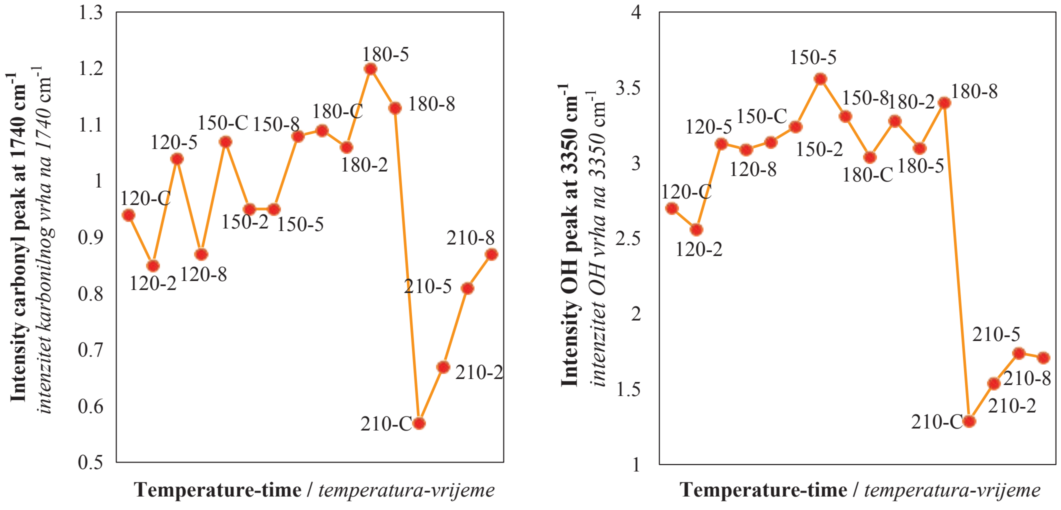

a) b)

Figure 6 a) Carbonyl group intensity of the 1740 cm^{-1} absorption band of cedar samples subjected to heat treatment at 120 150-180-210 °C for 2-5-8 hours b) Hydroxyl group intensity of the 3350 cm^{-1} absorption band of cedar samples subjected to heat treatment at 120-150-180-210 °C for 2-5-8 hour

Slika 6. a) Intenzitet karbonilne skupine apsorpcijske veze na 1740 cm^{-1} toplinski obrađenih uzoraka cedrovine na 120-150-180-210 °C tijekom 2-5-8 sati, b) intenzitet hidroksilne skupine apsorpcijske veze na 3350 cm^{-1} toplinski obrađenih uzoraka cedrovine na 120-150-180-210 °C tijekom 2-5-8 sati

esterification reactions. After esterification, the intensity of the carbonyl peak (Figure 6 a) increased. The highest increase was observed at 210 °C. Consequently, it was determined that the esterification reaction occurred more in the same samples of cedar wood at low temperatures due to the number of OH groups. The decrease in the intensity of accessible hydroxyl groups (Figure 6b) can be attributed to the formation of pre-existing cross-linking or the recrystallization of cellulose, which were determined to occur during heat treatment (Tjeerdsma and Militz, 2005). Esterification causes a decrease in the intensity of hydroxyl groups in the wood, resulting in a reduction in the intensity of the hydroxyl peak at 3350 cm^{-1} (Herrera *et al*., 2014). In another study, the observed decrease in peak intensity, indicative of hydroxyl (O-H) group stretching, was attributed to hemicellulose degradation (Haseli *et al*., 2024).

However, as the heating duration increases, this effect reverses, and either the decrease in hydroxyl absorption band intensity ceases or an increase is observed. This phenomenon can be explained by the depletion of reactants necessary for esterification and, more importantly, the formation of new hydroxyl groups due to the degradation of wood components (lignin, hemicellulose, and cellulose) (Esteves and Pereira, 2009; Brebu and Vasile, 2010; Výbohová *et al*., 2018; Taghiyari *et al*., 2020). While lignin degradation releases phenolic hydroxyl groups, carbohydrate degradation can also generate new hydroxyl groups. Additionally, changes in hydrogen bonding may influence the absorption band intensity. Under prolonged heating or at excessively high temperatures, charring may occur, leading to significant spectral changes (Boonstra and Tjeerdsma, 2006; Kim *et al*., 2014).

3.2 Contact angle measurement
3.2. Mjerenje kontaktnog kuta

In this research, some of the cedar wood samples were heat-treated, while others were not. Subsequently, contact angle measurements were conducted, and the properties of cedar wood samples with and without heat treatment were compared. These comparison results are shown in Figure 7.

When the contact angle θ is greater than or equal to 90°, the liquid tends to "ball up" on the surface, indicating poor wetting or low wettability and water-repellent properties. Conversely, when θ is less than 90°, the wettability of the surface increases (Friedrich, 2021; Krainer and Hirn, 2021). To investigate the effects of modification on cedar wood samples, contact angle measurements were performed using polar (water and glycerol) and non-polar (hexane) liquids. As shown in Figure 7, heat treatment decreased wettability with polar liquids but increased it with the non-polar liquid.

FTIR analyses provided a crucial foundation for understanding the chemical changes occurring in wood, as well as their effects on surface properties. Chemical transformations in lignin and hemicelluloses at high temperatures during heat treatment reduced the surface wettability of cedar wood, imparting an important property that can increase the material's water resistance. These changes are believed to result from processes such as the growth of cross-links between lignin and polysaccharides and the reduction of polar groups in the

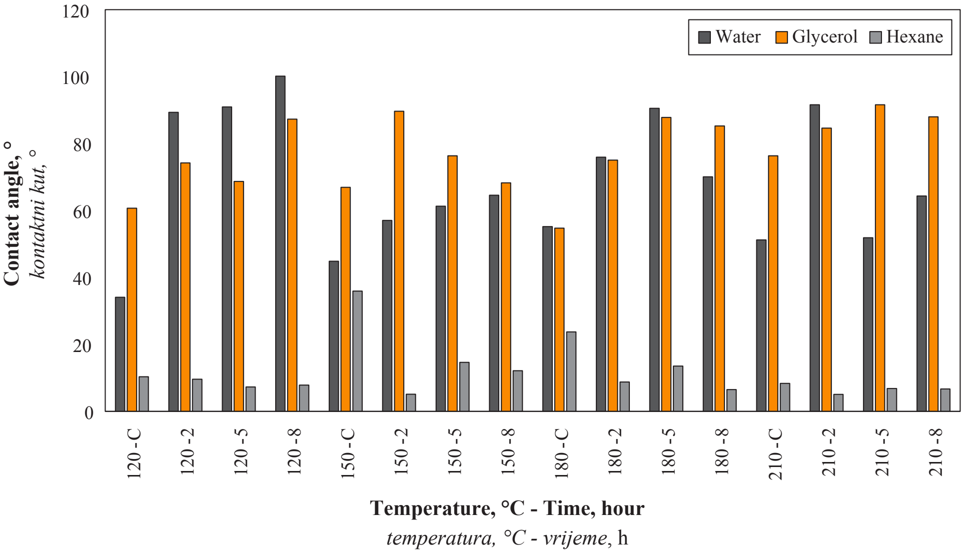

Figure 7 Contact angles of cedar wood samples after heat treatment depending on temperature and time
Slika 7. Kontaktni kutovi uzoraka cedrovine nakon toplinske obrade ovisno o temperaturi i vremenu

structure due to esterification reactions on the material's surface. The surface structures of wood materials differ from each other before and after heat treatment. This makes the differentiation of thermally treated/untreated samples very critical. In general, wood material is less wettable in polar solvents and more wettable in non-polar solvents after a heat treatment. Consequently, FTIR analyses have allowed for a general perspective for assessing the performance characteristics of cedar wood samples following the heat treatment, thus helping us to understand the polarity modifications emerging by the heat process (Gerardin *et al*., 2007; Budhe *et al*., 2020; Lovaglio *et al*., 2022).

These parameters were obtained from the contact angles of glycerol, hexane and water on cedar wood surfaces after heat treatment. The free surface energy values of the samples of polar-nonpolar and acidic-basic wood components were determined using these data according to the Lifshitz-van der Waals/acid-base (LW-AB) method (Mohammed-Ziegler *et al*., 2004; Gerardin *et al*., 2007; Qin *et al*., 2014).

According to other researchers, negative surface free energy values accompanied by high contact angles can occur due to the surface roughness of heat-treated wood samples, their chemically heterogeneous structure, and the limited penetration of the liquids used (Mohammed-Ziegler *et al*., 2004). Microscopic surface roughness can affect the determination of the contact angle due to the uncertainty of the real contact line, and the asymmetric arrangement cross asymmetrical arrangement of the multiple functional groups on the surface may lead to directional variations in the contact angle (Oss *et al*., 1988; Tadmor, 2004). Kung *et al*. (2019) have reported that topographical and chemical heterogeneities can exist at the micro and nanoscale that can induce non-ideal wetting and variability which, when not considered carefully, can be mistaken for true physical responses. Similarly, Alnoush *et al*. (2021) revealed that the wettability of calcite is distinctly affected by increasing surface roughness, which is not due to changes in the intrinsic surface energy, but to measurement artefacts. These effects are most prominent as the contact angles approach the detection limits, since small misfits in assumed droplet shape or im-

Table 3 Free energy components on the surfaces of heat-treated cedar wood samples at different temperatures and times
Tablica 3. Komponente slobodne površinske energije toplinski obrađenih uzoraka cedrovine pri različitim temperaturama i vremenima

Cedar wood samples *Uzorci cedrovine*	γ^{LW}	γ^{AB}	γ^{+}	γ^{-}	γ_{tot}
120 °C-control	0.22	(-)4.28	(-)1.08	4.25	4.06
120 °C 2 hour	(-)1.94	9.84	7.32	3.31	7.90
120 °C 5 hour	(-)2.34	9.60	8.44	2.73	7,26
120 °C 8 hour	(-)2.64	11.60	8.32	4.04	8,96
150 °C-control	3.83	(-)8.60	(-)3.88	4.77	(-)4.77
150 °C 2 hour	(-)1.51	5.25	1.18	5.86	3.74
150 °C 5 hour	(-)0.13	5.32	1.52	4.66	5.19
150 °C 8 hour	(-)0.62	6.95	3.19	3.78	6.33
180 °C-control	1.57	3.32	0.89	3.11	4,89
180 °C 2 hour	(-)1.59	8.89	5.09	3.89	7.3
180 °C 5 hour	(-)1.39	10.18	5.71	4.54	8.79
180 °C 8 hour	(-)1.75	8.42	3.56	4.99	6.67
210 °C-control	(-)0.75	4.00	0.81	4.95	3.25
210 °C 2 hour	(-)2.76	11.09	7.53	4.09	8.33
210 °C 5 hour	(-)1.05	1.94	(-)0.15	6.26	0.89
210 °C 8 hour	(-)1.52	7.10	2.31	5.46	5.58

aging inaccuracies can lead to substantial errors in energy calculations.

Another study observed that very weak repulsive interactions led to negative values on the interface (Hwang *et al*., 2011). Furthermore, as heat treatment alters the C-O-C stretching absorption band in the cellulose structure, other alterations in the material's surface characteristics might transpire. The adhesion process may be adversely affected by the reduction or alteration of this absorption band, which is typically absorbed in the 1050-1150 nm range (Garside *et al*., 2003).

One of the factors that significantly affects the contact angle is the presence of a chemically heterogeneous structure. As the volume of liquid drops on the substrate increases and the liquid drops move on the surface, water drops can be fixed on the surface due to the change in the chemicals on the surface of the material and, as a result, contact angles can be affected. At the same time, water drops can be fixed due to energy differences in the functional groups on the surface. Due to these reasons, liquid drops dropped on the surface are prevented from overcoming energy barriers and cause inaccurate measurement of contact angles (Cansoy *et al*., 2011; Yu *et al*., 2022).

According to the values in Table 3, significant increases occurred at 150 °C and 180 °C compared to 120 °C. This change was found to be consistent with the increases in the LW component after heat treatment in the study by Gérardin *et al*. (2007). However, LW values were negative at 210 °C and other temperatures due to the prolongation of the heat treatment time. This might be caused by unexpected structural variations on the materials' surface, such as modifications to the cellulose, lignin, and hemicellulose structures. Furthermore, surface free energy may rise while surface energy and polarity fall with longer heat treatment times. The substance may become more hydrophobic as a result of strong surface binding of molecules caused by this rise in surface free energy. At the same time, as it reduces the liquid surface area, it may suggest a strong molecular connection. According to Gerardin *et al*. (2007), Israelachvili (2011), and Vagli *et al*. (2024), all of these modifications may restrict the material's ability to interact with other chemicals.

The decrease in hydroxyl groups in cedar wood samples resulted in a drop in the 3350 cm^{-1} absorption band. This decline was particularly noticeable in cedar wood samples that were heated to 210 °C for two, five, and eight hours. This temperature shift indicates that the cellulose structure has begun to break down. Furthermore, depending on the temperature, the formation of water-loving groups like carbonyl groups may result in an additional drop in the density of hydroxyl groups.

There was a discernible change in the electron acceptor ($^{+}\gamma$) component when cedar wood samples were heated to 180 °C and 210 °C (Table 3). Depending on the heat treatment used, a considerable rise in the electron acceptor (γ^{+}) component was seen in a research by Gerardin *et al*. (2007). Wood material's capacity to absorb moisture is diminished as a result of decrease of hydrophilic OH groups caused by the modification process. Since heat treatment is generally effective at temperatures above 150 °C, no significant change was detected in the samples at 120 °C. However, it was determined that changes occurred in the samples as the temperature was kept constant and the heat treatment time increased. In this case, it can be argued that the beginning of modification of the samples was observed in the heat treatments of 2, 5 and 8 hours at 180 °C, as a result of the decomposition of hemicellulose structures, and reduction of the amorphous structures (Gerardin *et al*., 2007). Also, the period of modification started to slow down at 210 °C, as the cellulose structure began to disintegrate in the cedar wood samples.

During thermal treatment, the degradation of hemicellulose and the loss of hydrophilic functional groups (e.g., hydroxyl groups) decrease the surface water affinity and lead to a decrease in the electron donor component ($^{-}\gamma$) (Gao *et al*., 2022). At the same time, lignin molecules migrate towards the surface and the structure of lignin is rearranged, creating a more polar surface. This decrease in the electron acceptor component (γ^{+}) also contributes to a decrease in the overall surface energy (Rodriguez-Fabia *et al*., 2022). The remarkably low γtot value (0.89) of the sample after 5 h of heat treatment at 210 °C clearly demonstrates the effect of these mechanisms. Due to the large-scale destruction of hemicellulose and the condensation of lignin and cellulose, a polar and inert surface was formed, which reduced the energetic interactions of the surfaces and made it more hydrophobic (Gan *et al*., 2023). It was also noted that a significant decrease in acid-base properties was observed due to the presence of functional groups associated with the remaining lignin (Li *et al*., 2014).

The electron donor (γ^{-}) component increased at 120 °C for 2 h, 5 h and 8 h, at 150 °C for 5 h and 8 h and at 210 °C for 2 h. This can be explained by the chemical changes that occur as a result of heat treatment, which change the surface free energy of the material with different components. Such an increase in the surface free energy also causes a decrease in the contact angle. Moreover, amorphous hemicellulose molecules, such as xylose, mannose and arabinose, are degraded due to heat treatment. As a result of this degradation, there is an increase in crystallinity and lignin content (Gerardin *et al*., 2007).

4 CONCLUSIONS
4. ZAKLJUČAK

Upon analysis of heat-treated Taurus cedar samples, the decomposition of acetyl groups began at 180 °C and progressed notably when the temperature reached 210 °C, leading to a decreased content of acetyl groups that was more pronounced at the latter temperature.

Surface contact angle research revealed that heat treatment increased the wettability of non-polar molecules while decreasing that of polar ones. This decrease in wettability results from the removal of hydroxyl groups during the heat treatment process. The observed increase in electron acceptor component and van der Waals forces served as additional substantiation of the material alteration. Changes in the electron donor component under certain processing conditions revealed that hydrophilic groups had been eliminated.

The thermal modified Taurus cedar (*Cedrus libani*) wood (120-150 °C for 2 and 5 hours) has acquired improved properties suitable for the internal applications (as furniture and decorative coatings), the surface hydrophobicity and the structural stability. More intensive treatment (180-210 °C for 5 and 8 hours) further enhances water repellence, thus making the material compatible with outdoor applications (cladding, garden furniture). Nevertheless, the mechanical strength can decrease with the increase of the severity of the treatment, and therefore such materials are recommended for use in non-load-bearing applications. Optimizing heat treatment parameters plays an important role in improving the properties and service life of wood products. Moreover, research involving micro- and nano-scale modification, which aims to create superhydrophobic surfaces, is important for future increasing the durability and functionality of woody materials.

5 REFERENCES
5. LITERATURA

1. Adhikari, R.; Chanda, A.; Bakri, M. K. B.; Akinnuoye, M. M.; Peláez-Samaniego, M. R.; Aro, M.; Yadama, V., 2023: Performance of thermally modified wood strands and thin veneers for use in durable mass timber panels. Case Studies in Construction Materials, 23: e04920. https://doi.org/10.1016/j.cscm.2025.e04920
2. Alnoush, W.; Sayed, A.; Solling, T. I.; Alyafei, N., 2021: Impact of calcite surface roughness in wettability assessment: Interferometry and atomic force microscopy analysis. Journal of Petroleum Science and Engineering, 203: 108679. https://doi.org/10.1016/j.petrol.2021.108679
3. Altgen, M.; Kyyro, S.; Paajanen, O.; Rautkari, L., 2020: Resistance of thermally modified Scots pine sapwood against decay by the brown-rot fungus *Rhodonia placenta*. European Journal of Wood and Wood Products, 78 (153): 161-171. https://doi.org/10.1007/s00107-019-01482-z
4. Awoyemi, L.; Jones, I. P., 2011: Anatomical explanations for the changes in properties of western red cedar (*Thuja plicata*) wood during heat treatment. Wood Science and Technology, 45: 261-267. https://doi.org/10.1007/s00226-010-0315-9
5. Aydın, T. Y., 2021: Evaluation of heating temperature and time on bending properties of Taurus cedar wood. Turkish Journal of Forestry, 22 (4): 432-438. https://doi.org/10.18182/tjf.1019032
6. Aytin, A.; Çakıcıer, N.; Birtürk, T., 2022: Chemical, hygroscopic, and mechanical properties of various wood species heat treated via the ThermoWood® method. BioResources, 17 (1): 785-801. https://doi.org/10.15376/biores.17.1.785-801
7. Bal, B. C., 2013: Effects of heat treatment on the physical properties of heartwood and sapwood of cedrus Libani. BioResources, 8 (1): 211-219.
8. Barcik, S.; Gasparik, M.; Razumov, E. Y., 2015: Effect of thermal modification on the colour changes of oak wood. Wood Research, 60 (103): 385-396.
9. Barros Oliveira, C. A.; de Oliveira, K. A.; Borges de Moura Aquino, V.; Christoforo, A. L.; Molina, J. C., 2022: Characterization of Acrocarpus fraxinifolius wood submitted to heat treatment. Maderas. Ciencia y Tecnología, 24: 54. https://doi.org/10.4067/s0718-221x2022000100454_
10. Boonstra, M. J.; Tjeerdsma, B., 2006: Chemical analysis of heat-treated softwoods. European Journal of Wood and Wood Products, 64 (3): 204-211._https://doi.org/10.1007/s00107-005-0078-4
11. Boonstra, M., 2008: A two-stage thermal modification of wood. PhD Thesis in A plied Biological Sciences: Soil and Forest management. Henry Poincaré University, Nancy
12. Brebu, M.; Vasile, C., 2010: Thermal degradation of lignin:A review. Cellulose Chemistry & Technology, 44 (9): 353.
13. Budhe, S.; Banea, M. D.; Ghugal, S.; de Barros, S., 2020: Effects of heat treatment on the behavior of teak wood adherends bonded joints. Applied Adhesion Science, 8: 1-10. https://doi.org/10.1186/s40563-020-00124-5
14. Builes, H. J. F.; Sepulveda, V.; Osorio, J. A.; Ananias, R. A., 2021: Effect of thermal modification treatment on some physical and mechanical properties of *Pinus oocarpa* wood. Forests, 12 (68): 21-31. https://doi.org/10.3390/f12020249
15. Bytner, O.; Laskowska, A.; Drozdzek, M.; Kozakiewicz, P.; Zawadzki, J., 2021: Evaluation of the dimensional stability of black poplar wood modified thermally in nitrogen atmosphere. Materials, 14 (4): 149-161. https://doi.org/10.3390/ma14061491
16. Čabalová, I.; Výbohová, E.; Igaz, R.; Kristak, L.; Kačík, F.; Antov, P.; Papadopoulos, A. N., 2022: Effect of oxidizing thermal modification on the chemical properties and thermal conductivity of Norway spruce (*Picea abies* L.) wood. Wood Material Science & Engineering, 17 (5): 366-375. https://doi.org/10.1080/17480272.2021.2014566
17. Candelier, K.; Thevenon, M. F.; Petrissans, A.; Dumarcay, S.; Gerardin, P.; Petrissans, M.; 2016: Control of wood thermal treatment and its effects on decay resistance: A review. Annals of Forest Science, 73: 571-583. https://doi.org/10.1007/s13595-016-0541-x

18. Cansoy, C. E.; Erbil, H. Y.; Akar, O.; Akin, T., 2011: Effect of pattern size and geometry on the use of Cassie-Baxter equation for superhydrophobic surfaces. Colloids and Surfaces A: Physicochemical and Engineering Aspects, 386 (1-3): 116-124. https://doi.org/10.1016/j.colsurfa.2011.07.005
19. Caputo, D.; Fusco, C.; Nacci, A.; Palazzo, G.; Murgia, S.; D'Accolti, L.; Gentile, L., 2021: A selective cellulose/hemicellulose green solvents extraction from buckwheat chaff. Carbohydrate Polymer Technologies and Applications, 2: 100094. https://doi.org/10.1016/j.carpta.2021.100094
20. Chang, C. W.; Kuo, W. L.; Lu, K. T., 2019: On the effect of heat treatments on the adhesion, finishing and decay resistance of Japanese cedar (*Cryptomeria japonica* D. Don) and Formosa acacia (*Acacia confuse* Merr. (Leguminosae)). Forests, 10 (7): 586. https://doi.org/10.3390/f10070586
21. Chen, H.; Lang, Q.; Xu, Y.; Feng, Z.; Wu, G.; Pu, J., 2012: Effect of thermal treatment with methylolurea impregnated on poplar wood. BioResources, 7 (4): 5279-5289.
22. Chen, K.; Tan, Y.; Sun, F.; Zhu, J.; Peng, H.; Jiang, J.; Zhan, T., 2023: Influence of electrochemically deposited TiO_2 on the anti-weathering properties of heat-treated wood. Wood Material Science & Engineering, 18 (3): 801-809. https://doi.org/10.1080/17480272.2022.2071167
23. Chen, M.; Liu, X.; Yu, C.; Yao, M.; Xu, S.; Tang, W.; Gong, J., 2020: Strategy of selecting solvent systems for spherical agglomeration by the Lifshitz-van der Waals acid-base approach. Chemical Engineering Science, 220: 115613. https://doi.org/10.1016/j.ces.2020.115613
24. Cherdkeattikul, S.; Morisawa, Y.; Ida, T., 2020: Surface structural transformation of pre-carbonized solid biomass from Japanese cedar via ATR-FTIR and PCA. Analytical Sciences, 36 (6): 723-729. https://doi.org/10.2116/analsci.19P412
25. Chien, Y. C.; Yang, T. C.; Hung, K. C.; Li, C. C.; Xu, J. W.; Wu, J. H., 2018: Effects of heat treatment on the chemical compositions and thermal decomposition kinetics of Japanese cedar and beech wood. Polymer Degradation and Stability, 158: 220-227. https://doi.org/10.1016/j.polymdegradstab.2018.11.003
26. Cogulet, A.; Blanchet, P.; Landry, V., 2016: Wood degradation under UV irradiation: A lignin characterization. Journal of Photochemistry and Photobiology B: Biology, 158: 184-191. http://dx.doi.org/10.1016/j.jphotobiol.2016.02.030
27. Dassanayake, R. S.; Dissanayake, N.; Fierro, J. S.; Abidi, N.; Quitevis, E. L.; Boggavarappu, K.; Thalangamaarachchige, V. D.; 2023: Characterization of cellulose nanocrystals by current spectroscopic techniques. Applied Spectroscopy Reviews, 58 (3): 180-205. https://doi.org/10.1080/05704928.2021.1951283
28. De Ligne, L.; Fredriksson, M.; Thygesen, L. G., 2024: Influence of volatile degradation products from thermal wood modification on wood-water interactions. PREPRINT (Version 1) available at Research Square. https://doi.org/10.21203/rs.3.rs-5191132/v1
29. Dilik, T.; Hiziroglu, S., 2012: Bonding strength of heat treated compressed Eastern red cedar wood. Materials & Design, 42: 317-320. https://doi.org/10.1016/j.matdes.2012.05.050
30. Durmaz, E.; Ucuncu, T.; Karamanoglu, M.; Kaymakci, A., 2019: Effects of heat treatment on some characteristics of Scots pine (*Pinus sylvestris* L.) wood. BioResources, 14 (4): 9531-9543.
31. Esteves, B. M.; Pereira, H. M., 2009: Wood modification by heat treatment: A review. BioResources, 4 (1): 370-404.
32. Esteves, B.; Ferreira, H.; Viana, H.; Ferreira, J.; Domingos, I.; Cruz-Lopes, L.; Nunes, L., 2021: Termite resistance, chemical and mechanical characterization of Paulownia tomentosa wood before and after heat treatment. Forests, 12 (8): 1114. https://doi.org/10.3390/f12081114
33. Esteves, B.; Marques, A. V.; Domingos, I.; Pereira, H., 2007: Influence of steam heating on the properties of pine (*Pinus pinaster*) and eucalyptus (*Eucalyptus globulus*) wood. Wood Science and Technology, 41 (17): 193-207. https://doi.org/10.1007/s00226-006-0099-0
34. Esteves, B.; Pereira, H., 2008: Wood modification by heat treatment: A review. BioResources, 4(1): 370-404.
35. Esteves, B.; Velez Marques, A.; Domingos, I.; Pereira, H., 2013: Chemical changes of heat treated pine and eucalypt wood monitored by FTIR. Maderas. Ciencia y Tecnología, 15 (2): 245-258. https://doi.org/10.4067/S0718-221X2013005000020
36. Ferrari, M.; Ravera, F.; Rao, S.; Liggieri, L., 2006: Surfactant adsorption at superhydrophobic surfaces. Applied Physics Letters, 89 (5): 053104. https://doi.org/10.1063/1.2226771
37. Friedrich, D., 2021: Thermoplastic moulding of Wood-Polymer Composites (WPC): A review on physical and mechanical behaviour under hot-pressing technique. Composite Structures, 262: 113649. https://doi.org/10.1016/j.compstruct.2021.113649
38. Gaff, M.; Kubovský, I.; Sikora, A.; Kačíková, D.; Li, H.; Kubovský, M.; Kačík, F., 2023: Impact of thermal modification on color and chemical changes of African padauk, merbau, mahogany and iroko wood species. Reviews on Advanced Materials Science, 62 (1): 20220277. https://doi.org/10.1515/rams-2022-0277
39. Gan, J.; Chen, L.; Chen, Z.; Zhang, J.; Yu, W.; Huang, C.; Zhang, K., 2023: Lignocellulosic biomass□based carbon dots: synthesis processes, properties and applications. Small, 19 (48): 2304066. https://doi.org/10.1002/smll.202304066
40. Gao, Y.; Li, Y.; Ren, R.; Li, L.; Gao, J.; Chen, Y., 2022: Enhancing the mechanical properties and hydrophobicity of heat-treated wood by migrating and relocating sulfonated lignin. Holzforschung, 76 (7): 637-644. https://doi.org/10.1515/hf-2021-0207
41. Garside, P.; Wyeth, P., 2003: Identification of cellulosic fibres by FTIR spectroscopy – thread and single fibre analysis by attenuated total reflectance. Studies in Conservation, 48 (4): 269-275. https://doi.org/10.1179/sic.2003.48.4.269
42. Gérardin, P.; Petrič, M.; Petrissans, M.; Lambert, J.; Ehrhrardt, J. J., 2007: Evolution of wood surface free energy after heat treatment. Polymer Degradation and Stability, 92 (4): 653-657. https://doi.org/10.1016/j.polymdegradstab.2007.01.016
43. Gezici-Koç, Ö.; Erich, S. J.; Huinink, H. P.; Van der Ven, L. G.; Adan, O. C., 2017: Bound and free water distribution in wood during water uptake and drying as measured by 1D magnetic resonance imaging. Cellulose, 24: 535-553. https://doi.org/10.1007/s10570-016-1173-x

44. Gindl, M.; Sinn, G.; Gindl, W.; Reiterer, A.; Tschegg, S., 2001: A comparison of different methods to calculate the surface free energy of wood using contact angle measurements. Colloids and Surfaces A: Physicochemical and Engineering Aspects, 181 (1-3): 279-287. https://doi.org/10.1016/S0927-7757(00)00795-0
45. Godinho, D.; Ferreira, C.; Lourenço, A.; de Oliveira Araújo, S.; Quilhó, T.; Diamantino, T. C.; Gominho, J., 2024: The behavior of thermally modified wood after exposure in maritime/industrial and urban environments. Heliyon, 10 (3): e25020. https://doi.org/10.1016/j.heliyon.2024.e25020
46. González-Peña, M. M.; Curling, S. F., Hale, M. D., 2009: On the effect of heat on the chemical composition and dimensions of thermally-modified wood. Polymer Degradation and Stability, 94 (12): 2184-2193. https://doi.org/10.1016/j.polymdegradstab.2009.09.003
47. Gordobil Goñi, O., 2018: New products from lignin. PhD Thesis, University of the Basque Country, Spain.
48. Haseli, M.; Efhamisisi, D.; Abdulkhani, A.; Oladi, R.; Ungerer, B.; Al-Musawi, H.; Müller, U.; 2024: Effects of oil heat treatment on poplar wood properties: A pilot scale study. Construction and Building Materials, 430: 136353. https://doi.org/10.1016/j.conbuildmat.2024.136353
49. He, L.; Zhang, T.; Zhao, Y.; Zhao, X.; Hao, T.; Xu, K.; Yi, S., 2023: Contribution of tung oil to the resistance of heat-induced wood shrinkage during thermal modification. Industrial Crops and Products, 204: 117359. https://doi.org/10.1016/j.indcrop.2023.117359
50. Herrera, R.; Erdocia, X.; Llano-Ponte, R.; Labidi, J., 2014: Characterization of hydrothermally treated wood in relation to changes on its chemical composition and physical properties. Journal of Analytical and Applied Pyrolysis, 107: 256-266. http://dx.doi.org/10.1016/j.jaap.2014.03.010
51. Hill, C. A. S., 2007: Wood modification: chemical, thermal and other processes. John Wiley & Sons, Chichester.
52. Hill, C.; Altgen, M.; Rautkari, L., 2021: Thermal modification of wood: A review: Chemical changes and hygroscopicity. Journal of Materials Science, 56 (11): 6581-6614. https://doi.org/10.1007/s10853-020-05722-z
53. Hou, L.; Wu, P., 2019: Two-dimensional correlation infrared spectroscopy of heat-induced esterification of cellulose with 1, 2, 3, 4-butanetetracarboxylic acid in the presence of sodium hypophosphite. Cellulose, 26: 2759-2769. https://doi.org/10.1007/s10570-019-02255-w
54. Hwang, G.; Lee, C. H.; Ahn, I. S.; Mhin, B. J., 2011: Determination of reliable Lewis acid-base surface tension components of a solid in LW – AB approach. Journal of Industrial and Engineering Chemistry, 17 (1): 125-129. https://doi.org/10.1016/j.jiec.2010.12.009
55. Israelachvili, J. N., 2011: Intermolecular and Surface Forces, Academic Press.
56. Jaruwat, D.; Udomsap, P.; Chollacoop, N.; Fuji, M.; Eiad-Ua, A., 2018: Effects of hydrothermal temperature and time of hydrochar from Cattail leaves. In: Proceedings of 2nd International Conference on Science and Technology of Emerging Materials (STEMa), Pattaya, Thailand, 2018. Pattaya: STEMa2018, 020016. https://doi.org/10.1063/1.5053192
57. Jimenez, J. P.; Menadro, N. A.; Ramon, A. R.; Ponciano, S. M., 2011: Physico-mechanical properties and durability of thermally modified Malapapaya wood. Philippine Journal of Science, 140 (56): 13-23.
58. Kacik, F.; Luptáková, J.; Šmíra, P.; Nasswettrová, A.; Kačíková, D.; Vacek, V., 2016: Chemical alterations of pine wood lignin during heat sterilization. BioResources, 11 (2): 3442-3452.
59. Kamdem, D. P.; Pizzi, A.; Jermannaud, A., 2002: Durability of heattreated wood. Holz als Roh-und Werkstoff, 60(1): 1-6. https://doi.org/10.1007/s00107-001-0261-1
60. Kasemsiri, P.; Hiziroglu, S.; Rimdusit, S., 2012: Characterization of heat treated eastern redcedar (*Juniperus virginiana* L.). Journal of Materials Processing Technology, 212 (6): 1324-1330. https://doi.org/10.1016/j.jmatprotec.2011.12.019
61. Kaya, A. I.; Cifci, A.; Ilkucar, M., 2021: Use of Fourier transform infrared spectroscopy and artificial neural networks to predict the wood density of *Cedrus libani* A. Rich. Fresenius Environmental Bulletin, 30 (4): 3141-3148.
62. Khan, Z.; Javed, F.; Shamair, Z.; Hafeez, A.; Fazal, T.; Aslam, A.; Rehman, F., 2021: Current developments in esterification reaction: A review on process and parameters. Journal of Industrial and Engineering Chemistry, 103: 80-101. https://doi.org/10.1016/j.jiec.2021.07.018
63. Kim, J. Y.; Hwang, H.; Oh, S.; Kim, Y. S.; Kim, U. J.; Choi, J. W., 2014: Investigation of structural modification and thermal characteristics of lignin after heat treatment. International Journal of Biological Macromolecules, 66: 57-65. https://doi.org/10.1016/j.ijbiomac.2014.02.013
64. Kocaefe, D.; Poncsak, S.; Dor, G, V.; Younsi, R., 2008: Effect of heat treatment on the wettability of white ash and soft maple by water. Holz als Roh-und Werkstoff, 66 (5): 355-361. https://doi.org/10.1007/s00107-008-0233-9
65. Korkut, S.; Kocaefe, D.; 2009: Isıl işlemin odun özellikleri üzerine etkisi. Düzce Üniversitesi Ormancılık Dergisi, 5 (2): 11-34.
66. Krainer, S.; Hirn, U., 2021: Contact angle measurement on porous substrates: Effect of liquid absorption and drop size. Colloids and Surfaces A: Physicochemical and Engineering Aspects, 619: 126503. https://doi.org/10.1016/j.colsurfa.2021.126503
67. Kubovský, I.; Kačík, F., 2014: Colour and chemical changes of the lime wood surface due to CO_2 laser thermal modification. Applied Surface Science, 321: 261-267. https://doi.org/10.1016/j.apsusc.2014.09.124
68. Kubovský, I.; Kačíková, D.; Kačík, F., 2020: Structural changes of oak wood main components caused by thermal modification. Polymers, 12 (2): 485. https://doi.org/10.3390/polym12020485
69. Kung, C. H.; Sow, P. K.; Zahiri, B.; Mérida, W., 2019: Assessment and interpretation of surface wettability based on sessile droplet contact angle measurement: challenges and opportunities. Advanced Materials Interfaces, 6 (18): 1900839. https://doi.org/10.1002/admi.201900839
70. Li, M. Y.; Cheng, S. C.; Li, D.; Wang, S. N.; Huang, A. M.; Sun, S. Q., 2015: Structural characterization of steam-heat treated Tectona grandis wood analyzed by FT-IR and 2D-IR correlation spectroscopy. Chinese Chemical Letters, 26 (2): 221-225. https://doi.org/10.1016/j.cclet.2014.11.024
71. Li, N.; Chen, Y.; Yu, H.; Xiong, F.; Yu, W.; Bao, M.; Bao, Y., 2017: Evaluation of optical properties and chemical structure changes in enzymatic hydrolysis

lignin during heat treatment. RSC Advances, 7 (34): 20760-20765. https://doi.org/10.1039/c7ra02005h

72. Li, T.; Li, G.; Li, J.; Li, X.; Li, M.; Li, Y., 2024: Characterization of the odorous constituents and chemical structure of thermally modified rubberwood. Wood Material Science & Engineering, 19 (2): 442-450. https://doi.org/10.1080/17480272.2023.2255571
73. Li, W.; Wang, C.; Zhang, Y.; Jia, C.; Gao, C., Jin, J., 2014: The influence of hot compression on the surface characteristics of poplar veneer. BioResources, 9 (2): 2808-2823.
74. Liao, X.; Fang, X.; Gao, X.; Yi, S.; Zhou, Y., 2024: Effect of high-intensity microwave treatment on structural and chemical characteristics of chinese fir. Forests, 15 (3): 516. https://doi.org/10.3390/f15030516
75. Lovaglio, T.; D'Auria, M.; Gindl-Altmutter, W.; Lo Giudice, V.; Langerame, F.; Salvi, A. M.; Todaro, L., 2022: Thermal modification and alkyl ketene dimer effects on the surface protection of deodar cedar (*Cedrus deodara* Roxb.) wood. Forests, 13 (10): 551. https://doi.org/10.3390/f13101551
76. Lyu, J.; Wang, J.; Chen, M., 2024: Effects of heat treatment on the chemical composition and microstructure of *Cupressus funebris* Endl. wood. Forests, 15 (8): 1370. https://doi.org/10.3390/f15081370
77. Mastouri, A.; Azadfallah, M.; Rezaei, F.; Tarmian, A.; Efhamisisi, D.; Mahmoudkia, M.; Corcione, C. E., 2023: Kinetic studies on photo-degradation of thermally-treated spruce wood during natural weathering: Surface performance, lignin and cellulose crystallinity. Construction and Building Materials, 392: 131923. https://doi.org/10.1016/j.conbuildmat.2023.131923
78. Militz, H., 2002: Thermal treatment of wood European process and their background. International Research Group on Wood Preservation. Document no. IRG/WP 02-40241.
79. Mohammed-Ziegler, I.; Oszlánczi, Á.; Somfai, B.; Hórvölgyi, Z.; Pászli, I.; Holmgren, A.; Forsling, W., 2004: Surface free energy of natural and surface-modified tropical and European wood species. Journal of Adhesion Science and Technology, 18 (6): 687-713. https://doi.org/10.1163/156856104839338
80. Moosavinejad, S. M.; Madhoushi, M.; Vakili, M.; Rasouli, D., 2019: Evaluation of degradation in chemical compounds of wood in historical buildings using FT-IR and FT-Raman vibrational spectroscopy. Maderas. Ciencia y Tecnología, 21 (3): 381-392. https://doi.org/10.4067/S0718-221X2019005000310
81. Nabil, E.; Mahmoud, N.; Youssef, A.; Saber, E.; Kamel, S., 2018: Evaluation of physical, mechanical and chemical properties of Cedar and Sycamore woods after heat treatment. Egyptian Journal of Chemistry, 61 (6): 1131-1149. https://doi.org/10.21608/ejchem.2018.4301.1383
82. Peng, Q.; Ormondroyd, G.; Spear, M.; Chang, W. S., 2022: The effect of the changes in chemical composition due to thermal treatment on the mechanical properties of *Pinus densiflora*. Construction and Building Materials, 358: 129303. https://doi.org/10.1016/j.conbuildmat.2022.129303
83. Penvern, H.; Zhou, M.; Maillet, B.; Courtier-Murias, D.; Scheel, M.; Perrin, J.; Coussot, P., 2020: How bound water regulates wood drying. Physical Review Applied, 14 (5): 054051. https://enpc.hal.science/hal-03085702v1
84. Piernik, M.; Woźniak, M.; Pinkowski, G.; Szentner, K.; Ratajczak, I.; Krauss, A., 2022: Impact of the heat treatment duration on color and selected mechanical and chemical properties of scots pine wood. Materials, 15 (15): 5425. https://doi.org/10.3390/ma15155425
85. Qian, J.; Yue, K.; Liu, S.; Lu, D.; Wu, P.; Li, Q., 2024: Augmenting bamboo strength and thermal stability for sustainable construction. Journal of Cleaner Production, 451: 142073. https://doi.org/10.1016/j.jclepro.2024.142073
86. Qin, Z.; Chen, H.; Gao, Q.; Zhang, S.; Li, J., 2015: Wettability of sanded and aged fast-growing poplar wood surfaces: I. Surface free energy. BioResources, 10 (1): 1008-1023.
87. Qin, Z.; Gao, Q.; Zhang, S.; Li, S., 2014: Surface Free Energy and Dynamic Wettability of Differently Machined Poplar Woods. BiorResources, 9 (2): 3088-3103.
88. Rodriguez-Fabia, S.; Torstensen, J.; Johansson, L.; Syverud, K., 2022: Hydrophobisation of lignocellulosic materials. Part I: Physical modification. Cellulose, 29 (10): 5375-5393. https://doi.org/10.1007/s10570-022-04620-8
89. Rowell, R. M.; Ibach, R. E.; McSweeny, J.; Nilsson, T., 2009: Understanding decay resistance, dimensional stability and strength changes in heat treated and acetylated wood. In: Proceedings of European Conference on Wood Modification, April 27-29, Stockholm, Sweden, pp. 489-502. https://doi.org/10.1080/17480270903261339
90. Sandberg, D.; Kutnar, A.; Mantanis, G., 2017: Wood modification technologies: A review. Iforest-Biogeosciences and Forestry, 10 (6): 895-908. https://doi.org/10.3832/ifor2380-010
91. Sikora, A.; Kačík, F.; Gaff, M.; Vondrová, V.; Bubeníková, T.; Kubovský, I., 2018: Impact of thermal modification on color and chemical changes of spruce and oak wood. Journal of Wood Science, 64: 406-416. https://doi.org/10.1007/s10086-018-1721-0
92. Sivrikaya, H.; Ekinci, E.; Can, A.; Tasdelen, M.; Gokmen, K.; 2015a: Effect of heat treatment on the weathering and hardness properties of some wood species. In: Proceedings of the 11th Meeting of the Northern European Network for Wood Sciences and Engineering (WSE), Poland.
93. Srinivas, K.; Pandey, K. K., 2012: Effect of heat treatment on color changes, dimensional stability and mechanical properties of wood. Journal of Wood Chemistry and Technology, 32 (6): 304-316. https://doi.org/10.1080/02773813.2012.674170
94. Svensson, I.; Butron, A.; Puyadena, M.; González, A.; Irusta, L.; Barrio, A., 2023: Bio-based phosphate-containing polyester for improvement of fire reaction in wooden particleboard. Polymers, 15 (5): 1093. https://doi.org/10.3390/polym15051093
95. Tadmor, R., 2004: Line energy and the relation between advancing, receding and young contact angles. Langmuir, 20 (18): 7659-7664.
96. Taghiyari, H. R.; Bayani, S.; Militz, H.; Papadopoulos, A. N., 2020: Heat treatment of pine wood: Possible effect of impregnation with silver nanosuspension. Forests, 11 (4): 466. https://doi.org/10.3390/f11040466
97. Tjeerdsma, B. F.; Militz, H., 2005: Chemical changes in hydrothermal treated wood: FTIR analysis of combined hydrothermal and dry heat-treated wood. European Journal of Wood and Wood Products, 63 (2): 102-111. https://doi.org/10.1007/s00107-004-0532-8
98. Toba, K.; Nakai, T.; Saito, H., 2024: Effects of wood drying temperatures on the reduction in mechanical properties of Japanese cedar (*Cryptomeria japonica* D.

Don) perpendicular to grain. Buildings, 14 (9): 2624. https://doi.org/10.3390/buildings14092624

99. Tufan, M. Z.; Aydın, T. Y.; Güntekin, E.; Birol, Ü., 2022: Chemical properties of modified cedar wood. Turkish Journal of Forestry, 23 (4): 328-334. https://doi.org/10.18182/tjf.1140093
100. Tuncer, F. D.; Kartal, S. N.; Soytürk, E. E.; Arango, R. A.; Ohno, K. M.; Önses, M. S.; Ibanez, C. M., 2024: Changes in chemical properties and microstructure of *Pinus taeda* and *Eucalyptus bosistoana* woods modified by contact charring. European Journal of Wood and Wood Products, 82 (1): 107-121. https://doi.org/10.1007/s00107-023-02011-9
101. Vagli, G.; Tian, T.; Naef, F.; Jinno, H.; Celebi, K.; Santos, E. J.; Shih, C. J., 2024: Strong repulsive Lifshitz-van der Waals forces on suspended graphene. arXiv preprint, arXiv:2406.07384.
102. Van Oss, C. J.; Chaudhury, M. K.; Good, R. J., 1988: Interfacial Lifshitz-van der Waals and polar interactions in macroscopic systems. Chemical Reviews, 88 (6): 927-941.
103. Varga, D.; Tolvaj, L.; Molnar, Z.; Pasztory, Z., 2020: Leaching effect of water on photodegraded hardwood species monitored by IR spectroscopy. Wood Science and Technology, 54: 1407-1421.
104. Vidholdova, Z.; Kacík, C.; Reinprecht, L.; Cerova, V. K.; Luptakova, J., 2022: Changes in chemical structure of thermally modified spruce wood due to decaying fungi. Journal of Fungi, 8 (6): 739-750. https://doi.org/10.3390/jof8070739
105. Výbohová, E.; Kučerová, V.; Andor, T.; Balážová, Ž.; Veľková, V., 2018: The effect of heat treatment on the chemical composition of ash wood. BioResources, 13 (4): 8394-8408.
106. Wang, X.; Chen, X.; Xie, X.; Wu, Y.; Zhao, L., 2018: Effects of thermal modification on the physical, chemical and micromechanical properties of Masson pinewood (*Pinus massoniana* Lamb.). Holzforschung, 17 (2): 143-156.
107. Wang, Z. Y.; Hung, K. C.; Xu, J. W.; Liu, J. W.; Wu, Y. H.; Chang, W. S.; Wu, J. H., 2024: Physicomechanical properties of Japanese cedar wood modified by high-temperature vapour-phase acetylation (HTVPA), a simultaneous acetylation and heat treatment modification process. Journal of Industrial and Engineering Chemistry, 134: 271-280. https://doi.org/10.1016/j.jiec.2023.12.057
108. Wang, Z.; Yang, X.; Sun, B.; Chai, Y.; Liu, J.; Cao, J., 2016: Effect of vacuum heat treatment on the chemical composition of larch wood. BioResources, 11 (3): 5743-5750.
109. Wu, Z.; Deng, X.; Li, L.; Xi, X.; Tian, M.; Yu, L.; Zhang, B., 2021: Effects of heat treatment on interfacial properties of *Pinus Massoniana* wood. Coatings, 11 (5): 543. https://doi.org/10.3390/coatings11050543
110. Xu, J.; Zhang, Y.; Shen, Y.; Li, C.; Wang, Y.; Ma, Z.; Sun, W., 2019: New perspective on wood thermal modification: Relevance between the evolution of chemical structure and physical-mechanical properties and online analysis of release of VOCs. Polymers, 11 (1): 114-125. https://doi.org/10.3390/polym11071145
111. Yu, W.; Wang, M.; Wang, F.; Wang, X.; Wu, B., 2022: Study of the dynamic wetting behavior of Sn droplet impacting Cu substrate. Applied Physics A, 128 (8): 646. https://doi.org/10.1007/s00339-022-05795-4
112. Zhang, P.; Gao, J.; Liu, F.; Chen, Y.; Peng, Y., 2023: Study on the discoloration mechanism of Eucalyptus wood during thermal treatment in different media. Polymers, 15 (7): 1599. https://doi.org/10.3390/polym15071599
113. Zhang, X.; Shi, F.; Yu, X.; Liu, H.; Fu, Y.; Wang, Z.; Li, X., 2004: Polyelectrolyte multilayer as matrix for electrochemical deposition of gold clusters: toward superhydrophobic surface. Journal of the American Chemical Society, 126 (10): 3064-3065. https://doi.org/10.1021/ja0398722
114. Zhang, Y.; Xu, D.; Ma, L.; Wang, S.; Liu, X., 2017: Influence of heat treatment on the water uptake behavior of wood. BioResources, 12 (1): 1697-1705.
115. Zhao, T.; Jiang, L., 2018: Contact angle measurement of natural materials. Colloids and Surfaces B: Biointerfaces, 161: 324-330. https://doi.org/10.1016/j.colsurfb.2017.10.056
116. Zhu, L.; Liu, Y.; Liu, Z., 2016: Effect of high-temperature heat treatment on the acoustic-vibration performance of *Picea jezoensis*. BioResources, 11 (2): 4921-4934.
117. ***TAPPI T 558 om-97: Surface wettability and absorbency of sheeted materials using an automated contact angle tester.

Corresponding address:

MUHAMMED ZAKIR TUFAN
Department of Forest Products Engineering, Isparta University of Applied Sciences, Isparta, TURKEY,
e-mail: zakir_65@hotmail.com